Phase-space networks of geometrically frustrated systems

Yilong Han (韩一龙)

Department of Physics, Hong Kong University of Science and Technology, Clear Water Bay, Kowloon, Hong Kong

(Received 18 February 2009; revised manuscript received 26 September 2009; published 5 November 2009)

We illustrate a network approach to the phase-space study by using two geometrical frustration models: antiferromagnet on triangular lattice and square ice. Their highly degenerated ground states are mapped as discrete networks such that the quantitative network analysis can be applied to phase-space studies. The resulting phase spaces share some comon features and establish a class of complex networks with unique Gaussian spectral densities. Although phase-space networks are heterogeneously connected, the systems are still ergodic due to the random Poisson processes. This network approach can be generalized to phase spaces of some other complex systems.

DOI: 10.1103/PhysRevE.80.051102 PACS number(s): 05.50.+q, 64.60.aq, 75.10.Hk

I. INTRODUCTION

One challenge to understanding disordered solids is the complex geometry of their phase spaces, including the relative positions and interconnections between the different states. Phase spaces are usually too large and complicated to be directly studied. Here, we propose that some simple models of disordered solids, such as geometrical frustrated spin models, provide an ideal platform for phase-space studies. Geometrically frustrated systems have highly degenerated ground states with zero-point entropy [1]. Their whole phase spaces can be mapped as nontrivial complex networks, so that the recently developed large tool box of network analysis [2–4] can be used to understand phase spaces. On the other hand, these phase spaces provide a class of complex networks with unique topologies.

When a system has competing interactions, there is no way to simultaneously satisfy all interactions: a situation known as frustration. Frustration widely exists in systems ranging from neural networks to disordered solids. Frustration can also arise in an ordered lattice solely from geometric incompatibility [1]. For example, consider the three antiferromagnetic Ising spins on the triangle shown in Fig. 1(A). Once two of them are antiparallel to satisfy their antiferromagnetic interaction; there is no way that the third one can be antiparallel to both of the other two spins. Frustration leads to highly degenerated ground states and, subsequently, to complex materials with peculiar dynamics such as water ice [5], spin ice [6], frustrated magnets [6], artificial frustrated systems [7], and soft frustrated materials [8].

In geometrically frustrated systems, spins on lattices have discrete degrees of freedom, such that their phase spaces are discrete and can be viewed as networks. A node in the network corresponds to a state of the system. Two nodes are connected by an edge (i.e., a link) if the system can directly evolve from one state to the other without passing through intermediate states. Edges are undirected because dynamic processes at the microscopic level are time reversible. The challenge is how to construct and analyze such large phase-space networks. For example, how do we identify whether or not two nodes are connected?

II. ANTIFERROMAGNETS ON TRIANGULAR LATTICES AND SQUARE ICES

The first model we consider is antiferromagnetic Ising spins on a two-dimensional (2D) triangular lattice [9]. For a large system with periodic boundary conditions, it has $\sim e^{0.323N_{spin}}$ degenerated ground states, where N_{spin} is the number of spins [9]. For example, configuration 3A in Fig. 1(C) is one ground state in the hexagonal area. We refer to pairs of neighboring spins in opposite states, as satisfied bonds, i.e., they satisfy the antiferromagnetic interaction. Since one triangle has at most two satisfied bonds [see Fig. 1(A)], the ground state should have 1/3 of its bonds frustrated and 2/3 of its bonds satisfied [9]. If we plot only satisfied bonds, a ground state can be mapped to a random lozenge tiling [10] [see configuration 3A in Fig. 1(C)]. A lozenge is a rhombus with 60° angles. By coloring lozenges with different orientations with different gray scales; the tiling can be viewed as a stack of three-dimensional (3D) cubes, or as a simple cubic crystal surface projected in the [1] direction [10] [see Fig. 1(C)].

The ground state has a local zero-energy mode, as shown in Fig. 1(B): the central particle can flip without changing the energy since it has three up and three down neighbors. The system can evolve via a sequence of such single spin flips, even at zero temperature. We call such a local zero-energy mode as the *basic flip*. Any configuration change can be viewed as a sequence of such basic flips. Recently, we directly observed such flips in a colloidal monolayer [8]. In the language of cubes, a basic flip is equivalent to adding or removing a cube [see Fig. 1(B)]. By continuing to add or remove one cube from the stack surface, we can access all possible stack configurations in the large box. Thus, the ground-state phase space is connected at this "hexagonal boundary condition." The corresponding cube stacking in a large box is equivalent to the boxed plane partition problem in combinatorics [11]. The total number of ways to stack unit cubes in an L^3 box is given by the MacMahon formula [12],

$$N_n(L) = \prod_{1\le i,j,k\le L} \frac{i+j+k-1}{i+j+k-2} = \frac{H^3(L)H(3L)}{H^3(2L)} \sim \left(\frac{27}{16}\right)^{3/2L^2} \quad \text{when } L\to\infty, \quad (1)$$

where the hyperfactorial function $H(L)=\prod_{k=0}^{L-1}k!$. The first several $N_n(L=2,3,4,5,\ldots)$ are $20,980,232848,267227532,\ldots$ (see the number sequence A008793 in Ref. [13]). When $L=2$, all 20 ground-state configurations in Fig.

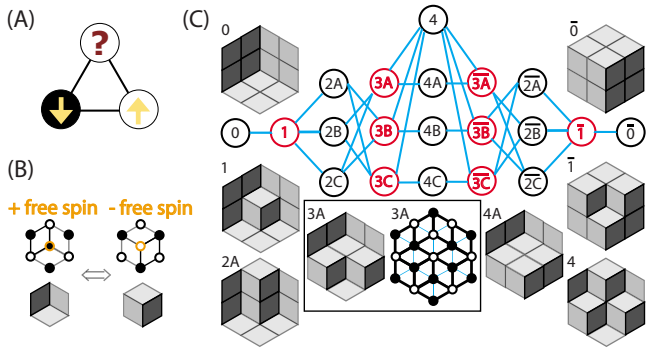

FIG. 1. (Color online) (A) Three antiferromagnetic spins on a triangle cannot simultaneously satisfy all their interactions. (B) The central spin has three up and three down neighbors, so that it can flip freely without energy change. Satisfied bonds can be viewed as cubes. The +/− free spin flip corresponds to adding/removing a cube. (C) The $2\times2\times2$ cube stacks are stable against gravity along the [1] direction. Stack configurations have one-to-one correspondence to Ising ground states under "hexagon boundary condition," e.g., see configuration 3A. In the right 3A configuration, the thick black lines are satisfied bonds forming rhombuses and the thin blue lines are frustrated bonds. In total, there are 20 legal stacks, i.e., 20 nodes in the phase-space network. The network is bipartite, i.e., consisting of alternating red (even number of cubes) and black (odd number of cubes) states.

1(C) have the same minimum possible energy, i.e., 12 frustrated bonds in 12 rhombuses. The 20-node phase-space network in Fig. 1(C) can be constructed based on the following two facts: (1) spins on lattice have discrete degrees of freedom, such that the phase space contains discrete number of microstate; (2) any configuration change can be decomposed to a sequence of basic flips. Consequently, we can define an edge between two nodes if the two states differ by only one basic flip (i.e., one cube), such that the system can *directly* change from one node to the other without passing through intermediate nodes. Note that multiple flips will *not* flip *exactly simultaneously* because time is continuous.

The ground-state phase-space networks of another frustration model known as the six-vortex model or square ice [14–16] can be similarly constructed. The ground state of the square ice follows the *ice rule*, i.e., each vertex has two incoming and two outgoing arrows. Flipping a closed loop of arrows from clockwise to counterclockwise (or vice versa) does not break the ice rule. The smallest four-arrow loops are basic flips since any configuration change can be decomposed as a sequence of such flips [15]. Similar to cube stacking, all the legal configurations of square ice under fixed boundary conditions are connected via basic flips [15]. In fact, the ground states of square ice have one-to-one correspondence to faced-centered cubic (FCC) stacks of spheres and different boundary conditions correspond to different container shapes [16]. The basic flip is equivalent to adding/removing a sphere [16]. Thus, both triangular antiferromagnets and square ice can be mapped to solid-on-solid (SOS) models: the former corresponds to simple cubic SOS and the latter corresponds to FCC SOS. The degeneracy of geometrical frustration strongly depends on boundary conditions [17]. For example, the number of $L\times L$ square ices with domain-wall boundary conditions is [18]

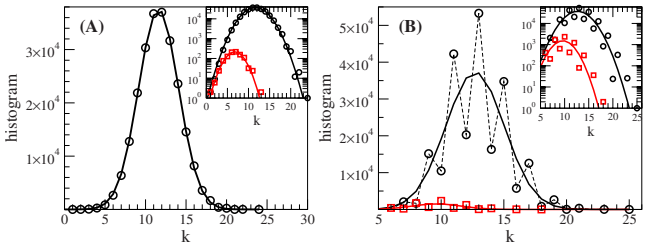

FIG. 2. (Color online) Connectivity distributions of ground-state phase-space networks. (A) Antiferromagnets on $L=4$ (circles) and $L=3$ (squares) triangular lattices at hexagon boundary conditions. (b) 7×7 (circles) and 6×6 (squares) square ices at domain-wall boundary conditions. Insets: semi-log plots. The curves in the main plots and insets show the best Gaussian fits.

$$N_n(L) = \prod_{1\le i\le j\le L} \frac{L+i+j-1}{2i+j-1} = \prod_{j=0}^{L-1} \frac{(3j+1)!}{(L+j)!}$$
$$\sim \left(\frac{27}{16}\right)^{L^2/2} \quad \text{when } L\to\infty, \tag{2}$$

i.e., the number of nodes of its phase-space network. This is much smaller than $N_n(L)\sim(64/27)^{L^2/2}$ when $L\to\infty$ under the periodic boundary condition [14].

In statistical physics, the two models we studied here are considered as exactly solvable [19] under periodic boundary conditions at the infinite-size limit. In contrast, combinatoric analysis yields exact results about finite systems at some fixed boundary conditions [e.g., Eqs. (1) and (2)]. The two models have been understood in exquisite detail through methods as varied as Bethe ansatz, Fermionic path integrals, field theories, etc., but few quantitative properties about phase spaces are known. Here we mapped out phase-space networks under free, periodic, and various fixed boundary conditions and found that they share some common features.

III. NETWORK PROPERTIES

We numerically studied phase-space networks of small triangular antiferromagnets and square ices under periodic, free, and various fixed boundary conditions. The phase space increases exponentially with the lattice size. Numerically, we can handle networks only up to 2 068 146 nodes and 13 640 060 edges (4×5 square ice under free boundary conditions); nevertheless, many general properties have emerged from such small systems.

The basic property of a network is the connectivity (or degree) distribution [4]. The connectivity k_i is the number of edges incident with the node i. The connectivities of two frustrated systems appear to have Gaussian-like distributions at larger system size (for example, see Fig. 2). We observed that this Gaussian behavior persists at other boundary conditions as well. This behavior is similar to that of small-world networks [4,20] and Poisson random networks [3,4] and different from that of scale-free networks [4,21]. Other network properties, such as the diameter and the cluster coefficient, can be readily derived from the cube/sphere stack picture. For cube stacks, the shortest path length between two nodes

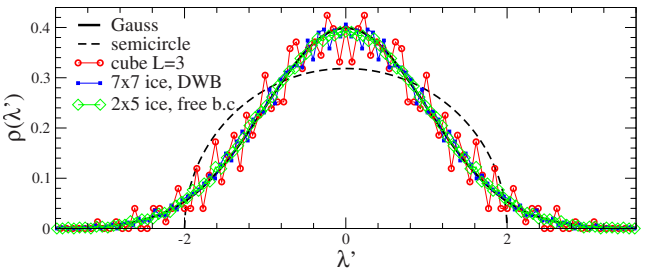

FIG. 3. (Color online) Spectral densities of phase-space networks. Variances are rescaled to 1 by $\lambda' = \lambda/\bar{k}^{-1/2}$. Black curve: Gaussian distribution $e^{-\lambda'^2/2}/\sqrt{2\pi}$. Dashed curve: Wigner's semicircle law for random networks. $\rho(\lambda) = \sqrt{4\sigma^2 - \lambda^2}/(2\pi\sigma^2)$ if $|\lambda| < 2\sigma$ and zero otherwise. The variance σ^2 is also rescaled to 1. Open circles: the spectral density of the 980-node network of $L=3$ cube stacks. Solid squares: the 7436-node network of 7×7 square ice under the domain-wall boundary condition. Open diamonds: 7782-node network of 2×5 square ice under the free boundary condition. Their Gaussian fits are indistinguishable from the black curve.

is simply the number of different sites among all the L^3 sites. The largest distance, i.e., the diameter of the network, is L^3 between the "vacant" and the "full" states. Here, we define the vacant state as no cube (i.e., L^3 vacant sites) and the full state as no vacant site (i.e., L^3 cubes). The networks have small-world properties [4,20] in the sense that the diameter L^3 is almost logarithmically small compared with the network size $\sim e^{N_{spin}} \sim e^{L^2}$. The network is bipartite [see the solid and open circles in Fig. 1(A)] because a cube stack comes back to its initial configuration only by adding and removing the same number of cubes, i.e., an even number of basic flips. Consequently, the cluster coefficient [4], which characterizes the density of triangles in the network, is 0.

Spectral analysis provides global measures of network properties. For an N_n-node network, the connectivity (or adjacent) matrix $\mathbf{A}$ is an $N_n \times N_n$ matrix with $A_{ij}=1$ if nodes i and j are connected, and zero otherwise. Since edges in phase-space networks are undirected, $\mathbf{A}$ is symmetric and all its eigenvalues λ_i are real. The spectral density of the network is the probability distribution of these N_n eigenvalues

$$\rho(\lambda) = \frac{1}{N_n}\sum_{i=1}^{N_n} \delta(\lambda - \lambda_i). \tag{3}$$

$\rho(\lambda)$'s qth moment M_q is directly related to the network's topological feature. $D_q = N_n M_q = \Sigma_{i=1}^{N} (\lambda_i)^q$ is the number of paths (or loops) that return back to the original node after q steps [4]. In a bipartite network, all closed paths have even steps so that all odd moments are zero. Consequently, the spectral density is symmetric and centered at zero. The ith node with k_i neighbors has k_i ways to return back after two steps; hence, the variance $\sigma^2 = M_2 = \Sigma_i k_i/N_n = \bar{k}$, where $\bar{k} = 2N_{edge}/N_n$ is the mean connectivity. We rescale the measured spectral densities by $\bar{k}^{1/2}$ to the unit variance (see Fig. 3). The rescaled spectral densities of different frustration models collapse onto the same *Gaussian* distribution.

We show that spectral densities are indeed Gaussian at the infinite-size limit. The characteristic function, i.e., the Fourier transform of the probability function, uniquely describes a statistical distribution. It can be written as a series of moments of the distribution. Hence, to prove that the spectral density is Gaussian, we only need to show that all orders of the moments are the same as those of a Gaussian distribution. For a Gaussian distribution centered at 0, its odd moments are zero and its even moments (of order q) are $M_q = \frac{(q)!}{2^{q/2}(q/2)!}\sigma^q = (q-1)!!\sigma^q$, where σ^2 is the variance. Here we count D_q in cube/sphere stacks and show that $M_q = D_q/N_n$ follows the Gaussian M_q at the infinite-size limit. We count D_{2n} by considering $2n$ basic flips $f_1, \bar{f}_1, f_2, \bar{f}_2, \ldots, f_n, \bar{f}_n$. Subscripts denote the time order and f_i must be earlier than its reverse flip $\bar{f}_i$. The $2n$ basic flips are placed in a $2n$-long sequence in time order. First, f_1 must be placed at step 1. Then, there are $2n-1$ choices for placing $\bar{f}_1$. Then, f_2 must be placed at the earliest available step (i.e., step 2 if $\bar{f}_1$ is not occupying that step). Then, $\bar{f}_2$ has $2n-3$ choices. Thus, in total, there are $(2n-1)!!$ legal sequences. Note that if f_i and f_j are flips of the same spin or neighbor spins, some sequences are illegal. However, the probability of such illegal case approaches 0 in infinitely large systems because a finite number of f_i's are diluted enough to be considered as independent. Next, we consider how many choices of f_i's there are. Given the initial state i, f_1 has k_i choices, f_2 has k_{i1} choices, $\ldots f_n$ has $k_{i(n-1)}$ choices. Here, k_{ij} is the connectivity of a node after walking j steps away from the initial node i. k_{ij} depends on the pathway of the j steps and is not a constant. In total, there are $\Pi_{j=0}^{n-1} k_{ij}$ choices. When the system size is large, $k_{ij} \simeq k_i \simeq \bar{k}$, where $\bar{k}$ is the number of free spins of the mean cube-stack surface. Here we use the fact that when the system size approaches the infinite-size limit, the dominant number of states is close to the mean SOS surface, i.e., the cube/sphere stack surface shape distribution peaks around this maximum possible surface and becomes like a Dirac delta distribution [22]. Consequently, the probability distribution of connectivity approaches a Dirac delta distribution as well. Combining the above results $D_{2n} \simeq \Sigma_{i=1}^{N_n}(2n-1)!!\Pi_{j=0}^{n-1} k_{ij} \simeq (2n-1)!!N_n\bar{k}^n$, which becomes exact at the infinite-size limit. Since $D_2 = N_n\bar{k} = N_n\sigma^2$, the $2n$th moment $M_{2n} = D_{2n}/N_n = (2n-1)!!\sigma^{2n}$, which are identical to the $2n$th moment of a Gaussian distribution. Odd orders of moment are all zero, which is identical to those of a Gaussian distribution centered at zero. Since all moments are identical to those of a Gaussian distribution, the spectral density of phase-space networks is Gaussian at the infinite-size limit. In fact, Fig. 3 shows that spectral densities are already very close to the Gaussian distribution when systems are not so large ($\sim 10^3$ nodes).

The Gaussian spectral density distinguishes phase spaces from other complex networks. For example, the spectral density of a random network is the semicircle in Fig. 3. The spectral densities have triangular distributions for scale-free networks and irregular distributions for small-world, modular hierarchical, and many real-world networks [23,24].

IV. POISSON PROCESSES AND ERGODICITY IN PHASE SPACES

Network analysis provides an opportunity to study ergodicity. Unlike billiards with deterministic trajectory, we assume that the spin flipping is due to the random thermal motion and does not depend on history. Thus, the dynamical evolution of the system can be viewed as a random walk on its phase-space network. It is still interesting to ask whether this random walk can uniformly visit each node given the complex structure in phase space and the complex frustration constrains in real space.

Random walks on a network are rather chaotic, and nodes with higher connectivities will be visited more frequently. Thanks to the theorem in Ref. [25], the mean visiting frequency for node i is k_i/N_{edge}, which only depends on local connectivity k_i, and does not depend on the global structure of the network. Here, N_{edge} is the total number of edges. This theorem is a direct consequence of the undirectedness of edges. Although highly connected nodes are visited more frequently ($\sim k_i$), interestingly, the equal-probability postulate does not break down because the average time stayed at node i is $\sim 1/k_i$. Basic flips are random and independent of history, meaning that it is a Poisson process. We define the flipping probability of a basic flip within a unit of time as ν, which is the intensity of the Poisson process. In Poisson processes, the time interval between flips (i.e., the staying time) has an exponential distribution $e^{-\nu t}$ and the mean staying time is $1/\nu$. For a node with connectivity k, the superposition of k Poisson processes is still a Poisson process with intensity $k\nu$ and, consequently, the mean staying time is $1/(k\nu)$. For example, the cube-stack configuration 4 in Fig. 1(C) has six free spins, while configuration 0 only has one free spin; hence, the mean lifetime of configuration 4 is 1/6 of that of configuration 0. A random walker has higher frequency ($\sim k$) to visit a high-k node but will stay there for a shorter time ($\sim 1/k$), so that the equal-probability postulate is recovered. The above analysis can be easily generalized to networks with weighted edges [26]. Boltzmann assumed that molecules shift from one microscopic configuration to the next in such a way that every possible arrangement is equally likely, i.e., all edges have the same weight. We found that the equal-probability postulate still holds if edges have different weights [16], which, for example, can represent different potential barriers in complex energy landscapes in phase spaces.

Note that the flipping dynamics of random tiling has been studied in Monte Carlo simulations [27,28]. In such discrete mathematical problems, it is natural not to take the staying time as Poisson random. Compared with the conventional random-walk simulations, the theorem of complex network [25] provides the *exact* result about visiting frequency for each node. This is also confirmed by our random-walk simulations. Moreover, conventional dynamic simulations explore a tiny portion of a huge phase space by random walks, while we map out the *whole* phase spaces of small systems so that exact results can be obtained from quantitative network analysis.

An ergodic system may be trapped in a small part of its phase space in a practical time scale. Such weak ergodicity can be *quantitatively* measured by the network community (or modular) analysis. In particular, spectral analysis can detect the network's community structures [31] if there are any. The algorithm in Ref. [31] can detect the network's community structures [31] if there are any, and the "strength" of each community is characterized by a number. We applied this algorithm [31] and identified some relatively highly connected subnetworks (i.e., communities). However, we still observe a number of edges between subnetworks. Simulations also show that the system can easily travel through the whole phase-space network via basic flips and will not be trapped in a local community for a long time. Hence, we consider the phase space as ergodic. Unlike 2D rhombus tiling, the flipping of 3D rhombus tiling has slowing-down dynamics due to entropic barriers [29]. Network community analysis can provide a way to quantify this weak ergodicity [30].

V. SUMMARY AND OUTLOOK

We mapped out the whole phase-space networks of small frustrated systems. From the numerical and theoretical analyses of the two models under different boundary conditions, we found that their phase-space networks share some universal features including the small-world property, Gaussian-like connectivity distributions, Gaussian spectral densities at the infinite-size limit, and the Poisson dynamics with equal probability on every node. Phase spaces are ergodic under free and fixed boundary conditions. Although the numerical results were obtained from small systems, they guided us to show that the above features are valid at the infinite-size limit. Compared with intensively studied social networks, information networks, biological networks, and technological networks [3], phase-space networks belong to a different class with unique topology characterized by Gaussian spectral densities.

The connections between geometrical frustration and complex networks provide new open questions and analysis tools. A large tool box has been developed since 1998 [20] to study complex network dynamics, correlations, centrality, community structures, fractal properties [32], coarse graining [33], etc. (see the recent review paper [4]). These tools can be readily applied to phase-space studies. For example, asymmetry in the random dynamic process is characterized by the potential-like network centrality [25], which has been confirmed in our simulation that the visiting frequencies of different states have a Gaussian-like distribution due to the Gaussian-like connectivity distribution. Network coarse-grain technique [33] can provide a quantitative method to coarse grain the phase space.

In particular, phase-space studies can cast lights on the highly controversial Tsallis nonextensive entropy [34,35], which is based on the assumption that nonequilibrium or long-ranged interacting systems have fractal phase spaces [34]. However, a real example to support this assumption was not available before. Since stacks of cubes or spheres have self-repeating patterns on various length scales in real space, their phase spaces might also be fractals. By applying the fractal analysis of complex network [32], we observed

that all the phase-space networks studied in this paper are fractals [36]. Indeed, geometrical frustrated ground states share the same features as the long-range interacting systems typically discussed in the context of Tsallis entropy. One example is the boundary effects, percolating through the entire system, so that the system is not uniform at the infinite-size limit [16,22] (i.e., cannot be called as thermodynamic limit) and cannot be viewed as a simple sum of its subsystems (i.e., nonextensive). On the other hand, the frustrated spin models are still ergodic because different nodes have different staying times. This is different from the systems discussed in the nonextensive entropy, which are usually nonergodic.

Phase-space structures are important for understanding the dynamics. However, they are usually too large and complicated so that quantitative analysis is hard. This paper only made another step toward this direction. Future research could provide more insights to other physical properties and reveal more general features about phase spaces of different systems at different temperatures. In fact, the phase-space networks can be similarly constructed for quasicrystals [22] with phason flips and for some other frustrated spin models with basic flips such as triangular and kagomé ices, antiferromagnets in 2D kagomé, and 3D pyrochlore lattices [1,15,37,38]. At finite temperatures, phase-space networks can be similarly constructed. The nodes are all configurations on the hypersurface in the phase space determined by the conservation laws, and the edges are the motions of basic flips and diffusion of thermal excitations.

ACKNOWLEDGMENT

We thank Michael Wong for helpful discussions.

[1] R. Moessner and A. R. Ramirez, Phys. Today **59**(2), 24 (2006).
[2] R. Albert and A.-L. Barabási, Rev. Mod. Phys. **74**, 47 (2002).
[3] M. E. J. Newman, SIAM Rev. **45**, 167 (2003).
[4] L. D. F. Costa, F. A. Rodrigues, G. Travieso, and P. R. Boas, Adv. Phys. **56**, 167 (2007).
[5] L. Pauling, J. Am. Chem. Soc. **57**, 2680 (1935).
[6] S. T. Bramwell and M. J. P. Gingras, Science **294**, 1495 (2001).
[7] R. F. Wang *et al.*, Nature (London) **439**, 303 (2006).
[8] Y. Han *et al.*, Nature (London) **456**, 898 (2008).
[9] G. H. Wannier, Phys. Rev. **79**, 357 (1950); Phys. Rev. B **7**, 5017(E) (1973).
[10] H. W. J. Blöte and B. Nienhuis, Phys. Rev. Lett. **72**, 1372 (1994).
[11] G. E. Andrews and K. Eriksson, *Integer Partitions* (Cambridge University Press, New York, 2004).
[12] G. E. Andrews, *Percy Alexander MacMahon: Collected Papers* (MIT Press, Cambridge, 1986), Vol. 2.
[13] http://www.research.att.com/~njas/sequences/
[14] E. H. Lieb, Phys. Rev. **162**, 162 (1967).
[15] K. Eloranta, J. Stat. Phys. **96**, 1091 (1999).
[16] Y. Han, e-print arXiv:0902.3158.
[17] R. P. Millane and N. D. Blakeley, Phys. Rev. E **70**, 057101 (2004).
[18] D. M. Bressoud, *Proofs and Confirmations: The Story of the Alternating-Sign Matrix Conjecture* (Cambridge University Press, New York, 1999).
[19] R. J. Baxter, *Exactly Solved Models in Statistical Mechanics* (Academic, London, 1982).
[20] D. J. Watts and S. H. Strogatz, Nature (London) **393**, 440 (1998).
[21] A.-L. Barabási and R. Albert, Science **286**, 509 (1999).
[22] N. Destainville, J. Phys. A **31**, 6123 (1998).
[23] I. J. Farkas, I. Derényi, A.-L. Barabási, and T. Vicsek, Phys. Rev. E **64**, 026704 (2001).
[24] M. A. M. de Aguiar and Y. Bar-Yam, Phys. Rev. E **71**, 016106 (2005).
[25] J. D. Noh and H. Rieger, Phys. Rev. Lett. **92**, 118701 (2004).
[26] A.-C. Wu, X.-J. Xu, Z.-X. Wu, and Y.-H. Wang, Chin. Phys. Lett. **24**, 577 (2007).
[27] D. B. Wilson, Ann. Appl. Probab. **14**, 274 (2004).
[28] N. Destainville, Phys. Rev. Lett. **88**, 030601 (2002).
[29] N. Destainville and V. Desoutter, Appl. Math. Inf. Sci. **2**, 83 (2008).
[30] N. Destainville (private communication).
[31] M. E. J. Newman, Proc. Natl. Acad. Sci. U.S.A. **103**, 8577 (2006).
[32] C. Song, S. Havlin, and H. A. Makse, Nature (London) **433**, 392 (2005).
[33] D. Gfeller and P. De Los Rios, Phys. Rev. Lett. **99**, 038701 (2007).
[34] A. Cho, Science **297**, 1268 (2002).
[35] C. Tsallis, *Introduction to Nonextensive Statistical Mechanics: Approaching a Complex World* (Springer, New York, 2009).
[36] Y. Peng and Y. Han (unpublished).
[37] R. Moessner and J. T. Chalker, Phys. Rev. B **58**, 12049 (1998).
[38] S. H. Lee *et al.*, Nature (London) **418**, 856 (2002).